Multisite phosphorylation of a CDK inhibitor sets a threshold for the onset of DNA replication

Piers Nash*†, Xiaojing Tang*†, Stephen Orlicky*, Qinghua Chen‡, Frank B. Gertler§, Michael D. Mendenhall‡, Frank Sicheri*‖, Tony Pawson*‖ & Mike Tyers*‖

** Programme in Molecular Biology and Cancer, Samuel Lunenfeld Research Institute, Mount Sinai Hospital, 600 University Avenue, Toronto M5G 1X5, Canada*
‡ L.P. Markey Cancer Center, Department of Biochemistry, University of Kentucky, Lexington, Kentucky 40536-0096, USA
§ Biology Department, Massachusetts Institute of Technology, Cambridge, Massachusetts 02139, USA
‖ Department of Medical Genetics and Microbiology, University of Toronto, 1 Kings College Circle, Toronto M5S 1A8, Canada
† These authors contributed equally to this work

SCF ubiquitin ligases target phosphorylated substrates for ubiquitin-dependent proteolysis by means of adapter subunits called F-box proteins. The F-box protein Cdc4 captures phosphorylated forms of the cyclin-dependent kinase inhibitor Sic1 for ubiquitination in late G1 phase, an event necessary for the onset of DNA replication. The WD40 repeat domain of Cdc4 binds with high affinity to a consensus phosphopeptide motif (the Cdc4 phospho-degron, CPD), yet Sic1 itself has many sub-optimal CPD motifs that act in concert to mediate Cdc4 binding. The weak CPD sites in Sic1 establish a phosphorylation threshold that delays degradation *in vivo*, and thereby establishes a minimal G1 phase period needed to ensure proper DNA replication. Multisite phosphorylation may be a more general mechanism to set thresholds in regulated protein–protein interactions.

Numerous regulatory proteins are targeted for degradation in a precisely programmed manner through the covalent conjugation of ubiquitin, which is transferred along a cascade of E1, E2 and E3 enzymes to the substrate[1]. Reiterative transfer of ubiquitin generates polyubiquitinated species that are recognized and rapidly degraded by the 26S proteasome. E3 enzymes, or ubiquitin ligases, catalyse the terminal step in ubiquitin transfer, and as such are the crucial determinants of substrate specificity. Substrate recognition depends on often ill-defined sequence elements, referred to as degrons, that are the binding sites for cognate E3 enzymes[1,2]. The E3–substrate interaction can be regulated at several levels. In some instances, limiting cofactors determine E3 activity, as in the case of the anaphase promoting complex/cyclosome (APC/C), which targets mitotic cyclins and other proteins for degradation during mitosis[3]. In other cases, E3 recognition depends on post-translational modification of the substrate. In particular, phosphorylation is often used to direct substrates to a recently described class of E3 enzymes termed Skp1–Cdc53/Cul1–F-box protein (SCF) complexes[3]. SCF complexes target a broad spectrum of substrates through a repertoire of substrate-specific adapter subunits called F-box proteins[4]. The 40-amino-acid F-box motif is a binding site for Skp1, which in turn links F-box proteins to a core ubiquitination complex composed of the scaffold protein Cdc53/Cul1, the RING-H2 domain protein Rbx1 (also known as Roc1 or Hrt1) and, usually, the E2 enzyme Cdc34 (ref. 3). F-box proteins capture phosphorylated substrates by means of carboxy-terminal protein–protein interaction regions, such as WD40 repeat domains or leucine-rich repeat (LRR) domains[5].

Cell cycle progression requires the precisely ordered elimination of cyclins and cyclin-dependent kinase (CDK) inhibitors by the ubiquitin system[3]. In yeast, commitment to division, called Start, requires a threshold level of G1 cyclins (Cln1/2/3), which serve to activate Cdc28 (also called Cdk1) in late G1 phase. As cells pass Start, B-type cyclin (Clb5/6)–Cdc28 kinases are activated, which is a necessary step for initiation of DNA replication[6]. The primary function of Cln–Cdc28 activity is to phosphorylate an inhibitor of the Clb–Cdc28 kinases called Sic1, thereby targeting it for degradation[6,7]. Phospho-Sic1 is specifically recognized by the F-box protein Cdc4, which recruits Sic1 for ubiquitination by the Cdc34–SCF complex[4,5,8]. Overexpression of stabilized forms of Sic1 that lack Cdc28 phosphorylation sites cause an arrest at the G1 phase[9], whereas deletion of *SIC1* causes premature DNA replication and rampant genome instability[10]. Cdc4 recruits several other substrates to the SCF core complex in a phosphorylation-dependent manner, including the Cln–Cdc28 inhibitor/cytoskeletal scaffold protein Far1, the replication protein Cdc6 and the transcription factor Gcn4 (ref. 3). In the mammalian cell cycle, SCF complexes target phosphorylated forms of cyclin E1 and the CDK inhibitor $p27^{Kip1}$ (refs 11, 12). The important role of SCF pathways is shown by the G1 phase arrest caused by non-phosphorylatable forms of $p27^{Kip1}$, and by the genome instability caused by expression of stabilized forms of cyclin E1 (refs 13, 14). In addition to cell cycle control, SCF-dependent proteolysis regulates the NFκB and Wnt/β-catenin signalling pathways, among others[15].

Despite the well documented requirement for substrate level phosphorylation in SCF-dependent ubiquitination, the mechanism by which phosphorylation drives substrate binding is unclear. On the one hand, for some substrates the binding interaction seems to be based on recognition of a phosphopeptide motif[16–18], in a manner that is analogous to phosphorylation-dependent recognition by Src homology 2 (SH2), phosphotyrosine-binding (PTB), 14-3-3 and forkhead-associated (FHA) domains[19]. On the other hand, degradation of substrates such as Sic1, Cdc6 or Cln2 seems to require phosphorylation on multiple, widely spaced sites[9,20,21]. Notably, alignment of the numerous genetically relevant phosphorylation sites in such substrates does not reveal an obvious consensus binding motif. To address the mechanism of Cdc4 substrate recognition, we surveyed a number of synthetic phosphopeptides derived from known substrates and identified a high-affinity consensus binding motif, termed the Cdc4 phospho-degron (CPD). The endogenous Cdc4 substrate Sic1 contains nine suboptimal CPD sites, at least six of which must be phosphorylated to allow recognition by Cdc4. This requirement for multisite phosphorylation not only imposes a threshold for Cln–Cdc28 kinase in late G1

phase, but may also confer switch-like characteristics on Sic1 degradation and subsequent entry into S phase.

Phosphorylation requirements in Sic1 recognition

Previous analysis has shown that multiple phosphorylation sites contribute to Sic1 ubiquitination *in vitro* and degradation *in vivo*[9]. To systematically determine the relative contributions of each of the nine CDK consensus sites in Sic1, we mutated each individual site and assessed the mutant proteins for stability *in vivo*, as well as for binding to Cdc4 *in vitro* (Fig. 1). Each of the mutant proteins inhibited Clb5–Cdc28 kinase activity to the same extent as wild-type Sic1, including Sic1^{0p}, which lacks all nine phosphorylation sites (Fig. 1b). Consistent with previous studies[9,22], conditional overexpression of *SIC1*^{T45A} from the *GAL1* promoter permanently arrested cells in G1 phase, whereas expression from the wild-type promoter caused a modest G1 delay (data not shown). Repression of the various *GAL1-SIC1* constructs in cells arrested at Start by mating pheromone allowed an estimate of Sic1 half-life *in vivo*, using a curve-fitting algorithm (Fig. 1c). Several phosphorylation sites contributed to Sic1 instability, with a rank order of Thr 45, Ser 76, Thr 5 and Thr 33, followed by less significant contributions from other sites. Analysis of binding of the panel of Sic1 mutants to Cdc4 indicated that no single site is required for recognition, although loss of either the Thr 45 or Ser 76 sites did diminish *in vitro* binding to some extent (Fig. 1d). We then determined which individual sites, or combinations thereof, are sufficient for degradation. Beginning with the Sic1^{0p} mutant, which lacks all nine CDK sites, we restored increasing numbers of phosphorylation sites and assessed the effects on viability and the Cdc4–Sic1 interaction. Serial reintroduction of the top-ranked five sites failed to restore Sic1 binding to Cdc4 or degradation *in vivo* (Fig. 1e, f). However, introduction of either of two combinations of six CDK phosphorylation sites or seven sites proved sufficient for Cdc4 binding *in vitro* and Sic1 degradation *in vivo* (Fig. 1e, f). Thus, efficient phosphorylation-dependent recognition by Cdc4 minimally requires six of the nine CDK phosphorylation sites in Sic1.

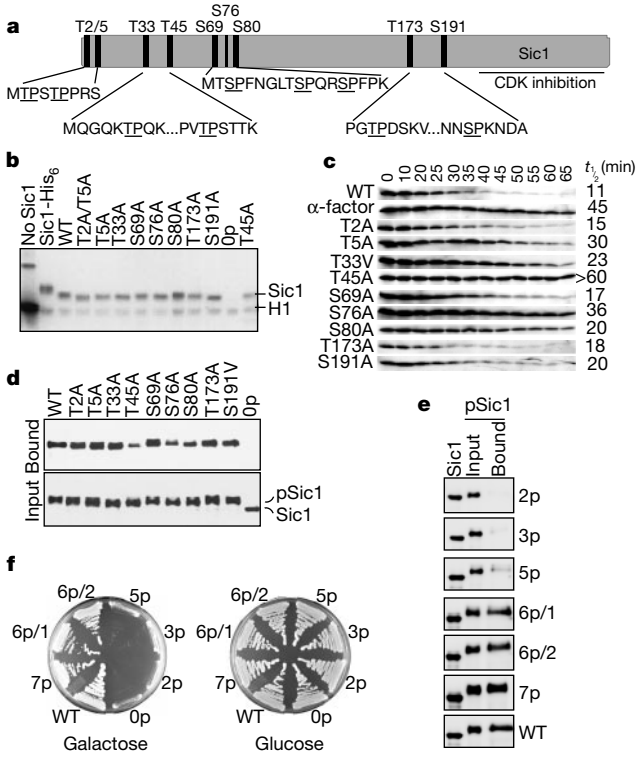

Figure 1 Contribution of CDK phosphorylation sites to Sic1 recognition, ubiquitination and degradation. **a**, Consensus S/T-P CDK phosphorylation sites in Sic1 (underlined). **b**, Inhibition of Clb5–Cdc28 kinase activity against histone H1 by purified Sic1 phosphorylation site mutants. WT, wild type. **c**, Half-life of Sic1 phosphorylation site mutants determined by decay of Sic1 protein on repression of *GAL1-SIC1*^{HA} constructs after release from α-factor arrest. The row labelled α-factor indicates decay rate of wild-type Sic1 before release. **d**, Binding of Sic1 phosphorylation site mutants to purified Cdc4. GST–Sic1 fusion proteins were phosphorylated by recombinant Cln2–Cdc28, captured onto Flag-tagged Cdc4 resin and detected with anti-Sic1 antibody. **e**, **f**, Phosphorylation of a minimum of six sites on Sic1 is required for interaction with Cdc4 *in vitro* (**e**) and degradation of Sic1 *in vivo* (**f**). Sites are indicated as follows: 2p = Thr 45, Ser 76; 3p = Thr 33, Thr 45, Ser 76; 5p = Thr 2, Thr 5, Thr 33, Thr 45, Ser 76; 6p/1 = Thr 2, Thr 5, Thr 33, Thr 45, Ser 69, Ser 76; 6p/2 = Thr 2, Thr 5, Thr 33, Thr 45, Ser 76, Ser 80; 7p = Thr 2, Thr 5, Thr 33, Thr 45, Ser 69, Ser 76, Ser 80. *GAL1-SIC1* strains were incubated for 2 days at 30 °C.

Identification of a Cdc4 phospho-degron

There are at least three possible modes of phospho-Sic1 binding to Cdc4. The first is a phosphorylation-dependent conformational change that exposes a pre-existing cryptic binding epitope on Sic1. The second is direct binding of multiple phosphorylated residues to multiple, distinct binding sites on Cdc4. The third mode is equilibrium binding of multiple phosphorylated residues on Sic1 with a single phospho-recognition site on Cdc4. To investigate these three different possibilities, we examined the ability of various synthetic phosphopeptides to bind to Cdc4 *in vitro* by fluorescence polarization. Phosphopeptides corresponding to sequences centred on Thr 45 of Sic1 or another candidate interaction site in Far1 (ref. 23) could neither bind to Cdc4 in this assay, nor block the interaction between full-length, phosphorylated substrates and Cdc4 (Fig. 2a, Table 1 and data not shown). We then surveyed other phosphopeptides and discovered that a 19-residue peptide centred on Thr 380 of mammalian cyclin E1 (CycE^{19pT380}), a site previously implicated in cyclin E1 degradation[24,25], bound to Cdc4 with high affinity. A biotinylated version of CycE^{19pT380}, but not the corresponding unphosphorylated peptide, was able to capture Cdc4 from lysates of insect cells infected with a recombinant baculovirus (see Supplementary Information). Fluorescence polarization measurements performed with CycE^{19pT380} and purified recombinant Cdc4 revealed an equilibrium dissociation constant (K_d) of 1.0 ± 0.05 μM and a Hill coefficient of 0.99 for the interaction, indicating a single class of high-affinity binding site on Cdc4 (Fig. 2b). The phosphorylated Thr 380 site in cyclin E1 also mediates Cdc4 recognition within the context of the intact protein, as full-length cyclin E1 is targeted for degradation by SCF^{Cdc4}, both *in vitro* and *in vivo* (see Supplementary Information). Importantly, the CycE^{19pT380} phosphopeptide was able to out-compete both Cdc4 binding and ubiquitination of cyclin E1, Sic1 and Far1 (Fig. 2a and data not shown). Thus, the CycE^{19pT380} peptide binds the same site(s) on Cdc4 as its fully phosphorylated, physiological substrates.

The CPD consensus

To identify the principal phosphopeptide determinants for Cdc4 recognition, a peptide Spots array technique was used[26]. Each position of the CycE^{19pT380} peptide was systematically altered to each of the 20 natural amino acids in a membrane-array format. Interaction of purified Skp1–Cdc4 complex with peptides on the membrane was detected with an anti-Skp1 antibody (Fig. 2c). Several characteristics of the binding site were revealed by the peptide array analysis. First, phosphorylated threonine (pThr) and a Pro at the +1 position are strictly required, consistent with the specificity of the targeting CDK kinases. Second, binding specificity is contributed by sequences that are amino-terminal to the phosphorylation site as there is a strong selection for Leu, Ile or Pro at the −1 position, whereas only Leu or Ile are preferred at the −2 position. Third, and quite unexpectedly, Arg and Lys residues seem to be disfavoured at the +2 to +5 positions, as is Tyr to a lesser extent. The optimal substrate selectivity of Cdc4 is therefore at odds

with that of the cognate targeting kinase Cdc28, which strongly prefers to phosphorylate S/T-P sequences followed by C-terminal basic residues[27].

The peptide Spots analysis was verified by quantitative fluorescence polarization measurements with various derivatives of the CycE^{19pT380} phosphopeptide (Table 1). The minimal peptide sequence required for binding was delimited to a core recognition sequence, LLpTPP, which bound Cdc4 with a K_d of 0.85 ± 0.1 μM. Introduction of basic residues in the +2 to +5 positions caused a decrease in solution binding affinity, most notably at the +2 and +3 positions, in conformity to the sequence preference for phosphorylation directed by CDK enzymes. The detrimental effect of basic residues is mediated by positive electrostatic potential because placement of an acetylated lysine at the +3 position yielded wild-type binding affinity. Finally, the essential pThr residue was strongly preferred over pSer (Table 1), suggesting an additional level of complexity in substrate discrimination. For brevity, we refer to the consensus binding sequence, L/I-L/I/P-pT-P⟨RK⟩$_4$, as the CPD motif, where ⟨X⟩ refers to disfavoured residues.

Physiological CPD motifs bind over a wide range of affinities

Database searches revealed that the CPD motif is present in numerous yeast proteins, including a recently characterized SCF^{Cdc4} substrate—the yeast transcriptional activator Gcn4 (ref. 28). Notably, one of the relevant targeting phosphorylation sites on Gcn4, Thr 165, is embedded in a sequence that closely matches the CPD consensus, and a phosphopeptide centred on Thr 165 of Gcn4 bound to Cdc4 with a K_d of 0.88 ± 0.1 μM (Table 1). When the Gcn4 peptide sequence was permuted in a Spots array, the resulting consensus binding sequence closely matched that derived from cyclin E1 (Fig. 2d). The Gcn4 sequence seems to be exquisitely tuned for Cdc4 binding, as variations in the principal CPD residues at positions −2 and −1 are not tolerated as well as they are in the core cyclin E1 motif. By the same token, residues at the +2 to +5 positions appear less important, presumably because the core region binds more tightly. Another known Cdc4 substrate, Far1, also contained two reasonable matches to the CPD motif, but not within regions previously implicated in Far1 degradation[23,29]. Sequences centred on Thr 63 and Thr 306 matched the CPD motif, and indeed a phosphopeptide centred on Thr 306 bound weakly to Cdc4 (Table 1). Phosphorylation of this site seems to contribute to activation of Far1 by the MAP kinase Fus3 (ref. 30), raising the possibility that Far1 activation is directly coupled to its recognition by SCF^{Cdc4}. To directly compare the relative affinities of

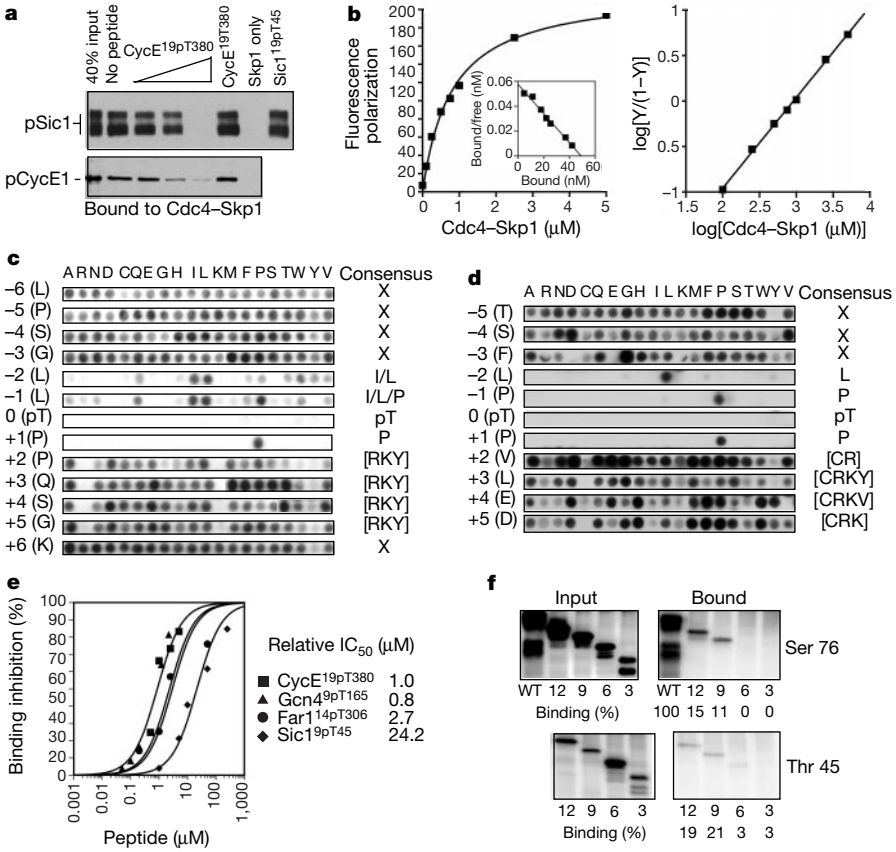

Figure 2 A phosphopeptide derived from cyclin E1 defines a high-affinity binding site on Cdc4. **a**, A CycE^{19pT380} phosphopeptide (ASPLPSGLLpTPPQSGKKQS), but not a Sic1^{19pT45} phosphopeptide, out-competes binding of phospho-Sic1 and phospho-cyclin E1 to Cdc4. The indicated peptides (3, 17 and 68 μM for CycE^{19pT380}; 68 μM for CycE^{19T380} and Sic1^{19pT45}) and phosphoproteins were incubated with Flag-tagged Skp1–Cdc4 resin. Bound proteins were detected with anti-Sic1 and anti-cyclin E1 antibodies. **b**, Michaelis–Menton plot (left), Scatchard plot (inset) and Hill plot (right) for the CycE^{19pT380} phosphopeptide interaction with Skp1–Cdc4 as measured by fluorescence polarization. **c**, **d**, Delineation of the CPD consensus with membrane-bound arrays of synthetic peptides based on the CycE^{13pT380} sequence (**c**) or the Gcn4^{11pT165} sequence (**d**). Each residue in the seed sequence (vertical axis) was substituted with every natural amino acid (horizontal axis). Membranes were incubated with purified Skp1–Cdc4 complex followed by detection with anti-Skp1 antibody. **e**, Peptide half-maximal inhibitory concentration (IC_{50}) curves for competition of fluorescein-CycE^{9pT380} peptide away from Cdc4 by CycE^{19pT380}, Gcn4^{9pT165}, Far1^{14pT306} or Sic1^{9pT45}. **f**, Concatamerization of low-affinity CPD motifs generates a high-affinity interaction with Cdc4. Varying numbers of suboptimal CPD sites corresponding to sequences derived from either a mixed Sic1 S76/S80/T5S site (GLTSPQRSPFPKSSPPRS) or the Sic1 T45 site (VTPSKPVTPSKPVTPSR) were produced as GST fusion proteins, phosphorylated by Cln2/Cdc28 in the presence of [^{32}P]-γ-ATP, captured onto Flag-tagged Cdc4 resin and detected by autoradiography. Capture efficiencies were normalized to that of phospho-Sic1.

several CPD-containing peptides, we used a competition binding assay with a fluorescein-labelled CycE^{9pT380} peptide. Under these conditions, it was possible to detect weak binding of a Sic1^{9pT45} peptide, demonstrating that weak CPD sites can mediate a direct interaction with Cdc4. Other natural CPD sequences bound with various affinities in the rank order Gcn4^{9pT165} ≥ cyclin E^{19pT380} > Far1^{21pT306} ≫ Sic1^{9pT45} (Fig. 2e).

Concatamers of weak CPDs bind Cdc4 with high affinity

To test the possibility that the multiple, weak phospho-dependent interaction motifs in Sic1 might act in concert to form a high-affinity phospho-Sic1–Cdc4 complex, we tested artificial substrates that carried increasing numbers of weak CPD sites derived from Sic1. Glutathione *S*-transferase (GST) fusion proteins were constructed with 3, 6, 9 or 12 CDK phosphorylation sites, with the reiterated sequences corresponding to either an artificial fusion of the Ser 76, Ser 80 and Thr 5 (substituted to Ser) sites of Sic1, or to a variant form of the Thr 45 site with a disfavoured Lys residue substituted at the +3 position. The purified fusion proteins were phosphorylated with Cln2–Cdc28 kinase in the presence of [^{32}P]-γ-ATP and assayed for Cdc4 binding. Although fusion proteins tagged with three or six weak CPD sites proved incapable of interacting with Cdc4, those with 9 or 12 sites were efficiently captured by Cdc4 (Fig. 2f). All non-phosphorylated versions of the GST–CPD fusions failed to interact with Cdc4 (data not shown). It is unlikely that the two different polymers of weak CPD sites fold into a defined tertiary structure; indeed, circular dichroism studies suggest that in its unphosphorylated form Sic1 lacks any detectable higher-order structure (see Supplementary Information). On the basis of these results, we conclude that the Sic1–Cdc4 interaction is directly mediated by a series of low-affinity CPD sites.

CPD interactions with the WD40 domain

Deletion analysis of Cdc4 demonstrated that the WD40 repeat domain is sufficient for high-affinity interaction with the CycE^{19pT380} peptide (Fig. 3a). In all known cases, direct phospho-dependent interactions are mediated by Arg and Lys residues[31]. To identify potential CPD binding sites, we modelled the Cdc4 WD40 repeat sequence onto the β-transducin WD40 structure[32], and mapped eight Arg residues conserved between Cdc4 and its homologues from *Candida albicans* and *Schizosaccharomyces pombe* onto the predicted β-propeller structure (Fig. 3b and Supplementary Information). Each Arg residue was individually mutated to Ala, and the resulting mutants were tested for their ability to rescue Cdc4 function in a plasmid shuffle experiment. Three substitutions abrogated Cdc4 function *in vivo* (R467A, R485A and R534A), whereas the other five mutations did not alter growth rate (Fig. 3c). Recombinant R467A, R485A and R534A mutant proteins were severely compromised for binding to both the CycE^{19pT380} peptide and phosphorylated Sic1 protein, whereas the neutral mutation, R443A, did not alter binding (Fig. 3d, e). Thus, consistent with the single class of high-affinity binding site identified by fluorescence polarization, we have found a single, localized interaction region in Cdc4. We speculate that the triad of essential Arg residues may comprise a phospho-Thr binding pocket.

A single, optimal CPD efficiently targets Sic1

To test whether an optimal CPD can function in a heterologous context, we inserted the cyclin E1 peptide motif or derivatives thereof into the Sic1^{0p} mutant. When the CycE^{19pT380} sequence was placed at the Thr 45 site of Sic1^{0p} (Sic1$^{T45::CycE19T380}$), it was able to confer recognition and ubiquitination by SCF^{Cdc4} *in vitro* (Fig. 4a, b), and elimination of Sic1^{0p} *in vivo* (Fig. 4c). Mutation of the

Table 1 Affinities of phosphopeptides for Cdc4

Peptide name	Peptide sequence	K_d (μM)
Effect of peptide length		
CycE^{19pT380}	ASPLPSGLLpTPPQSGKKQS	1.0 ± 0.08
CycE^{16pT380}	ASPLPSGLLpTPPQSGK	0.9 ± 0.1
CycE^{9pT380}	GLLpTPPQSG	1.0 ± 0.05
CycE^{5pT380}	LLpTPP	0.85 ± 0.1
Effect of pT		
CycE^{9pT380}	GLLpTPPQSG	1.0 ± 0.05
CycE^{9pT380S}	GLLpSPPQSG	6.0 ± 0.9
CycE^{9pT380Y}	GLLpYPPQSG	ND
CycE^{9pT380}	GLLTPPQSG	ND
Cost of basic residues		
CycE^{9pT380}	GLLpTPPQSG	1.0 ± 0.05
CycE$^{9pT380/L378K}$	GKLpTPPQSG	12 ± 2
CycE$^{9pT380/L379K}$	GLKpTPPQSG	6.0 ± 1.2
CycE$^{9pT380/P381A}$	GLLpTAPQSG	ND
CycE$^{9pT380/P381K}$	GLLpTPKQSG	6.3 ± 1.2
CycE$^{9pT380/Q382K}$	GLLpTPPKSG	5.1 ± 1.4
CycE$^{9pT380/Q382K(Ac)}$	GLLpTPPK(Ac)SG	1.0 ± 0.1
CycE$^{9pT380/S384K}$	GLLpTPPQKG	4.3 ± 1.3
CycE$^{9pT380/G385K}$	GLLpTPPQSK	2.4 ± 0.8
Other phosphopeptides		
CycE^{9pT380}	GLLpTPPQSG	1.0 ± 0.05
Gcn4^{9pT165}	FLPpTPVLED	0.88 ± 0.1
Far1^{20pT63}	PKPLNLSKPIpSPPPSLKKTA	ND
Sic^{9pT45}	VPVpTPSTTK	ND
Far1^{14pT306}	TGEFPQFpTPQEQLI	~25 ± 6
p27^{9pT187}	VEQpTPKKPG	ND

Results are the average of at least three individual sets of fluorescence polarization readings. Errors are s.e.m. of all measurements. Values for which saturation binding could not be achieved are indicated as approximate (~). ND indicates no binding detected by fluorescence polarization up to a Skp1–Cdc4 concentration of 10 μM. pT, phosphorylated threonine.

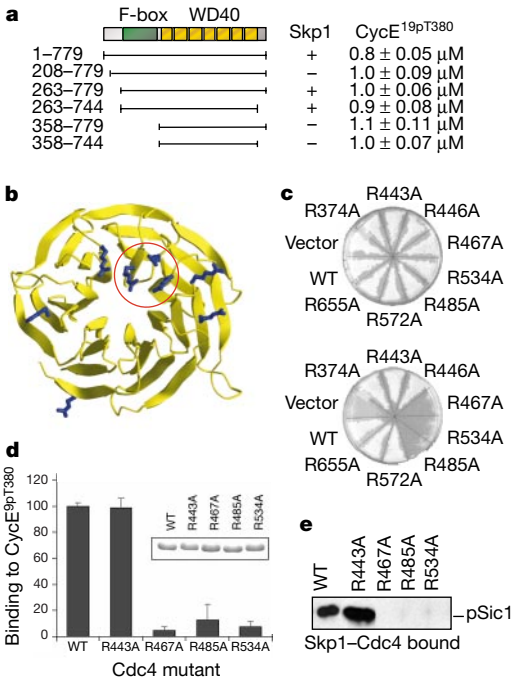

Figure 3 Identification of a CPD binding site on Cdc4. **a**, Equilibrium binding constants for the Cdc4–CycE^{19pT380} interaction determined by fluorescence polarization for a series of Cdc4 deletion mutants. Skp1 binding to Cdc4 was determined by anti-Skp1 immunoblot. **b**, Ribbons diagram of α-carbon chain of the β-propeller structure of the WD40 repeat region of β-transducin. Conserved Arg residues in Cdc4 are superimposed at predicted positions. The cluster of three Arg residues critical for Cdc4 function and peptide binding is circled in red. An alignment of Cdc4 homologues is provided in Supplementary Information. **c**, Mutation of any one of three conserved Arg residues (R467A, R485A, R534A) abolishes Cdc4 function *in vivo*. *CDC4* alleles on a *TRP1 ARS CEN* plasmid were transformed into a *cdc4Δ* strain containing a *CDC4 URA3 CEN* plasmid and plated on either Trp$^-$Ura$^-$ (top) or 5-FOA medium (bottom) for 2 days at 30 °C. **d**, **e**, Interaction of Cdc4 WD40 repeat region mutants with CycE^{9pT380} peptide measured by fluorescence polarization (**d**) and phospho-Sic1 detected by anti-Sic1 antibody (**e**). Equal levels of soluble protein were tested (inset).

Thr 380 residue completely eliminated recognition, demonstrating that the heterologous targeting was dependent on phosphorylation. To exclude the possibility that the inserted 19 residues might unduly contort Sic1 and allow recognition in an unnatural context, we substituted the core CPD around either the Thr 45 or Ser 76 sites, without introduction of additional residues. Substitution of the LLpTPP sequence at the Ser 76 site of Sic1^{0p} conferred effective phosphorylation-dependent ubiquitination *in vitro* and degradation *in vivo*, indicating that this single, minimal motif is sufficient for Cdc4 recognition in the context of full-length Sic1 (Fig. 4). The analogous substitution at the Thr 45 site conferred more modest recognition and incomplete ubiquitination and permanent growth arrest on overexpression. Furthermore, conversion of the residues flanking Thr 45 into an optimal CDK recognition sequence did not allow Sic1 recognition *in vitro*, or degradation *in vivo* (Fig. 4). We infer that additional local context effects must influence recognition of the CPD motif. Nonetheless, the fact that an appropriately positioned optimal CPD is sufficient to target Sic1 for degradation *in vivo* raises the question as to why the cell instead relies on multiple, suboptimal CPD sites to eliminate Sic1.

Suboptimal CPDs set a threshold for Sic1 degradation

We sought to test whether the multiple, weak CPD sites in Sic1 are important for biological function. To this end, we introduced a version of Sic1 that lacked seven of the endogenous CDK phosphorylation sites but that incorporated a single, high-affinity LLTPP motif in place of Ser 76 (Sic1$^{2p\text{-}S76LLTPP}$, hereafter referred to as Sic1^{CPD}), at the chromosomal *SIC1* locus under the control of the endogenous *SIC1* promoter. As Sic1 is needed to link DNA replication to other events at Start[7], we compared the onset of DNA replication in wild-type and *SIC1^{CPD}* strains on synchronous release from a G1-phase α-factor arrest. To expand the pre-replicative window, cells were grown under suboptimal nutrient conditions. Unlike wild-type cells, which delay all events at Start under these conditions, *SIC1^{CPD}* cells are unable to restrain DNA replication (Fig. 5a). Importantly, Sic1^{CPD} exhibits identical CDK inhibitory activity to that of the wild-type protein (Fig. 5b), indicating that the biological effects of the optimal CPD arise from defective regulation of Sic1 stability. As the Sic1^{CPD} protein proved difficult to detect in wild-type cells, we arrested *SIC1 cdc28-13* and *SIC1^{CPD} cdc28-13* strains at the restrictive temperature of 37 °C to inactivate Cdc28 kinases. Sic1^{CPD} was readily detected in the *cdc28-13* arrested cells, and on release to the permissive temperature of 25 °C it decayed with a faster onset than wild-type Sic1 (Fig. 5c). Degradation of Sic1^{CPD} was also advanced in early G1 phase populations obtained by elutriation (data not shown). We considered the possibility that targeting of Sic1^{CPD} is rewired to depend on other kinases, such as the CDK enzyme Pho85 (ref. 33), which prefers hydrophobic residues at the +2 position[34]. However, overexpression of the Pho85-specific cyclin Pcl2 did not affect accumulation of Sic1^{CPD} in *cdc28-13* arrest. Furthermore, Sic1^{CPD} was phosphorylated by Cln2–Cdc28 or Pcl2–Pho85 kinases, and dephosphorylated by the Cdc14 phosphatase, with similar efficiency to that of wild-type Sic1 *in vitro* (data not shown).

As experiments based on cell populations can obscure events at the individual cell level through averaging effects[35], we compared the properties of Sic1 and Sic1^{CPD} in single cells by use of green fluorescent protein (GFP) fusions[36]. Early-G1-phase cells bearing *SIC1–GFP* or *SIC1^{CPD}–GFP* alleles integrated at the chromosomal locus were obtained by centrifugal elutriation. The wild-type Sic1–GFP fusion was detected in all but the largest G1 phase cells, and was absent in all budded cells (Fig. 5d). This result at the level of the single cell is consistent with previous studies on cell cycle regulation of Sic1 abundance in synchronized cultures[6,7,37]. In contrast, the Sic1^{CPD}–GFP fusion was detected at variable levels and only in a fraction of the elutriated G1 population. As expected, the Sic1^{CPD} mutant was absent from all budded cells. The variable abundance of Sic1^{CPD}–GFP was also evident in G1 cells from unperturbed asynchronous cultures (Fig. 5d). These observations suggest that the optimal CPD site causes precocious and uncoordinated elimination of Sic1.

Premature DNA replication leads to genome instability in both yeast and mammalian cells[10,14], presumably because incomplete origin assembly leads to defective genome replication in S phase. Genome stability was measured in wild-type and *SIC1^{CPD}* strains by determining rates of chromosome loss in a colony colour-sectoring assay (Fig. 5e). The rate of chromosomal loss was increased by approximately 100-fold in the *SIC1^{CPD}* strain, an effect comparable to that observed for other mutants defective in chromosome transmission[38]. The pivotal function of Sic1 in the maintenance of genomic integrity is underscored by the massive rate of chromosome loss in a *sic1Δ* strain (Fig. 5e). Sic1 also has a crucial function at the end of mitosis, where it facilitates elimination of Clb–Cdc28 activity to re-establish G1 phase, as shown by the inviability of strains that lack both Sic1 and the APC/C activator Cdh1 (ref. 3). As predicted, we failed to recover *SIC1^{CPD} cdh1Δ* double mutants from a cross between *SIC1^{CPD}* and *cdh1Δ* strains (Fig. 5f). This result also indicates that mitotic forms of CDK activity are competent to target Sic1 for degradation through the optimal CPD motif.

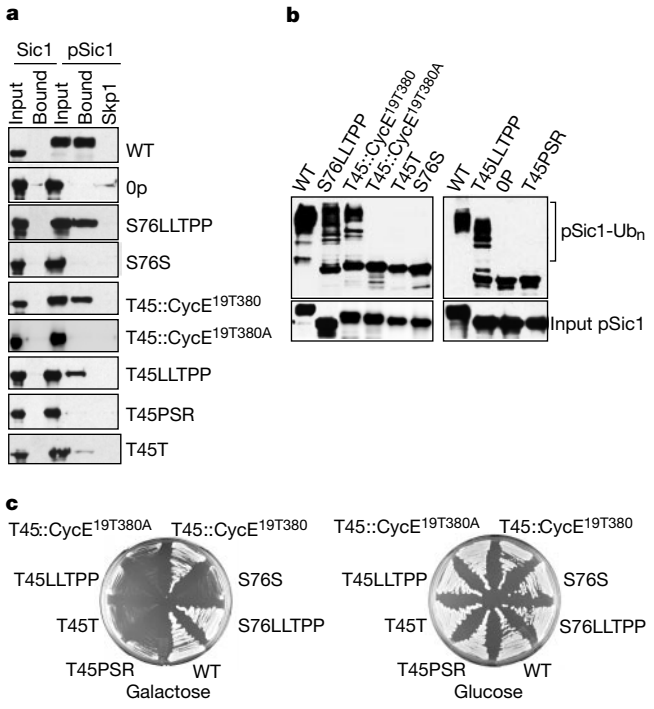

Figure 4 A single, optimal CPD motif is sufficient to target Sic1 to Cdc4. **a**, Capture by Cdc4 of Sic1^{0p} bearing a CycE^{19pT380} insert at Thr 45 or the core CPD motif (LLpTPP) substituted at either Thr 45 or Ser 76. T380A indicates the corresponding non-phosphorylatable insertion; T45PSR indicates a mutant in which the Thr 45 site is converted to an optimal CDK phosphorylation site; S76S and T45T indicate single wild-type sites reintroduced into Sic1^{0p}. GST–Sic1 fusion proteins were either unmodified or phosphorylated by Cln2–Cdc28 and captured on Flag-tagged Skp1–Cdc4 or, as a control, Flag-tagged Skp1 resin. Inputs shown are 40% of total and detection was with anti-Sic1 antibody. **b**, SCF^{Cdc4}-mediated ubiquitination of the same set of Sic1 mutants as in **a**. **c**, Insertion of the CycE^{19pT380} sequence at Thr 45 or substitution of the CPD core motif at Ser 76 restores degradation *in vivo*. *GAL1-SIC1* strains were incubated for 2 days at 30 °C.

Optimal versus suboptimal CPD motifs

The consensus binding site for the WD40 repeats of Cdc4 contains three main determinants. The first is an absolute requirement for

phospho-Ser/Thr followed by a Pro residue. The second is a strong preference for Leu and Ile residues in the −2 position and Pro, Leu or Ile residues in the −1 position. The final requirement is a bias against basic residues in the +2 to +5 positions. Given the minimal experimentally determined CPD, LLpTPP, it is apparent why inspection of many known phosphorylation sites implicated in targeting various substrates to Cdc4 has failed to yield an obvious consensus sequence. In particular, the nine CDK sites in Sic1 are all non-optimal CPD motifs in that a basic residue is present in the +2 to +5 positions, or a Thr phosphorylation site is replaced with a lower-affinity Ser site, or the −1 and −2 positions lack the preferred hydrophobic residues. Similarly, the eight CDK phosphorylation sites that influence Cdc6 recognition by Cdc4 lack one or more features of an ideal CPD[20,39,40]. The apparent low affinity of each individual site in Sic1 for Cdc4 explains the requirement for multisite phosphorylation. Given the evidence suggesting a single coincident CPD and substrate-binding site on Cdc4, the strong interaction between phospho-Sic1 and Cdc4 is most easily explained by a high, local concentration of low-affinity binding sites, which effectively drive the equilibrium towards complex formation. The apparent ability of SCF complexes to multimerize might also potentiate high-affinity interactions *in vivo*[41].

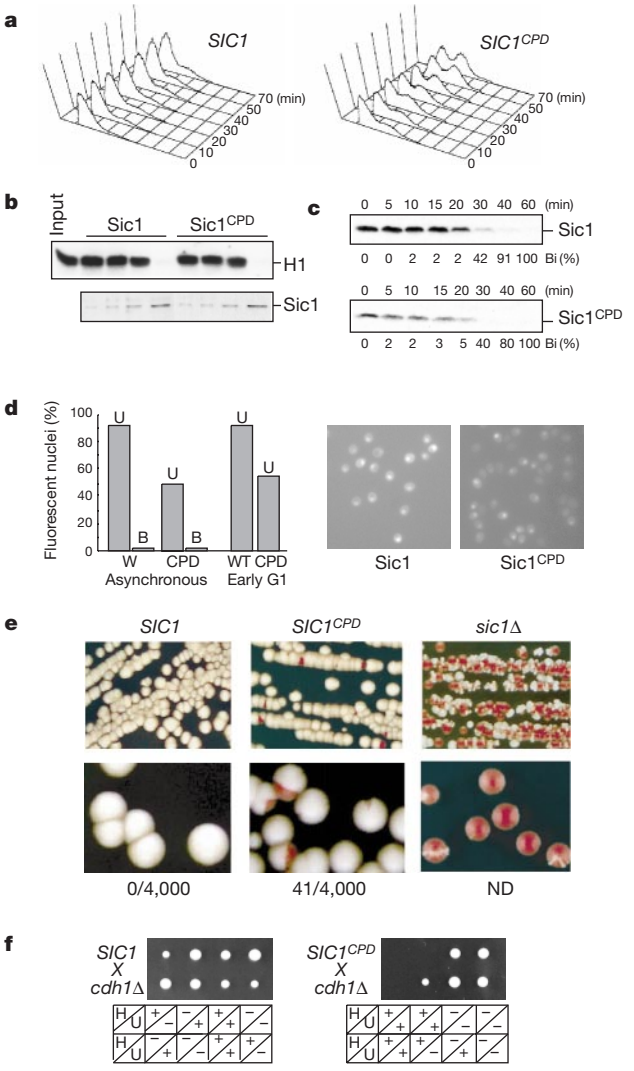

Figure 5 Premature DNA replication and genome instability caused by a single, optimal CPD motif. **a**, Strains bearing integrated wild-type *SIC1* or *SIC1*$^{2p\text{-}S76LLTPP}$ (*SIC1*^{CPD}) alleles were synchronized in G1 phase with α-factor, released into raffinose medium at 25 °C and assessed for total DNA content by FACS analysis. **b**, CDK inhibitory activity of Sic1 and Sic1^{CPD} measured against recombinant Clb5–Cdc28 complexes. At the highest concentration shown, both wild-type Sic1 and Sic1^{CPD} are in slight stoichiometric excess of Clb5. **c**, Premature onset of Sic1^{CPD} protein instability *in vivo*. Strains bearing a *cdc28-13* allele and either wild-type *SIC1* or the *SIC1*^{CPD} allele were incubated at 37 °C for 2 h, released at 25 °C and immunoblotted for total Sic1 protein. Bi, per cent of budded cells. **d**, Analysis of Sic1– and Sic1^{CPD}–GFP fusion protein levels in individual cells. Asynchronous cultures or early-G1-phase populations obtained by centrifugal elutriation were assessed for nuclear fluorescence in unbudded (U) and budded (B) cells. Representative fields are shown for G1-phase populations. **e**, Genome instability caused by the *SIC1*^{CPD} allele. Strains carried a marker chromosome that confers an Ade$^+$ phenotype (white colonies); red sectors indicate a chromosome loss event. Primary chromosome loss events were determined by scoring 4,000 individual colonies for red sectors that formed approximately 50% of the colony mass. ND, not determined. **f**, Synthetic lethal interaction between *cdh1Δ* and the *SIC1*^{CPD} allele. H and U indicate deduced His and Ura prototrophy. Of 66 tetrads from the *SIC1*^{CPD}*-URA3* cross, 46 His$^+$ Ura$^+$ spore clones did not form colonies, whereas 19 formed small colonies that could not be propagated. Of 31 tetrads from the *SIC1-URA3* cross, two His$^+$ Ura$^+$ spore clones did not form colonies, whereas 20 formed colonies that could be stably propagated.

There can be no absolute mechanistic requirement for multiple phosphorylation sites in substrate recognition by Cdc4, as it is capable of efficiently capturing substrates that bear a single, high-affinity CPD motif. Despite this observation, it seems probable that most physiological substrates of Cdc4 are recognized by multiple, low-affinity CPD sites. Although Gcn4 degradation depends in part on the strong CPD site centred on Thr 165 (ref. 28), it has recently been shown that multiple CDK sites contribute to Gcn4 degradation[42]; notably, all of these other sites occur within sub-optimal matches to the CPD. Two other Cdc4 substrates, Far1 and Ash1, also seem to require phosphorylation on multiple sites for efficient Cdc4 recognition (M.T., X.T. and Q. Liu, unpublished data). Similarly, the LRR-containing F-box protein Grr1 targets Cln2 for degradation in a manner that is dependent on multisite phosphorylation[5,21,43]. The possible generalization of this theme awaits careful investigation of binding interactions between metazoan F-box proteins and their substrates.

Multisite phosphorylation and biological thresholds

Identification of the CPD sequence has uncovered an unexpected mechanism in phosphorylation-dependent protein interactions, in which kinase specificity and phosphopeptide recognition can be antagonistic, as opposed to cooperative, parameters. A dynamic balance between phosphorylation and recognition by the ubiquitination machinery could provide flexibility in substrate degradation to allow fine-tuning of irreversible regulatory switches, such as those that occur in cell cycle transitions. In late G1 phase, a threshold level of Cln1/2–Cdc28 activity is required to activate events associated with Start, including elimination of Sic1 (refs 7, 9). If, on average, phosphorylation on a single site led to the immediate degradation of Sic1, then small fluctuations in CDK activity would erode the ability of the pool of Sic1 to restrain Clb-Cdc28 activity, potentially leading to an uncoordinated onset of DNA replication. Although a single, optimal CPD motif in Sic1 results in recognition by Cdc4, and consequent ubiquitination and degradation, it does not allow precise control of Start, but rather causes precocious S-phase onset and chromosomal instability. That is, the single CPD motif fails to set an appropriate threshold for S phase because it is recognized too efficiently. In contrast, degradation of wild-type Sic1 demands phosphorylation of at least six out of nine CDK sites, thereby imposing a much higher kinase threshold. In this sense, Sic1 integrates Cln–Cdc28 activity, and potentially other G1 phase kinases[33,44], to act as a timing device for G1 phase.

Multisite phosphorylation is a common feature of many protein kinase substrates, and yet its biological role has remained enigmatic in most instances. Phosphorylation on multiple residues may help enable events such as multisite docking interactions, integration of different kinase pathways, substrate dephosphorylation, subcellular localization, and protein activity[45]. Perhaps most importantly though, multisite phosphorylation occurs within a cellular

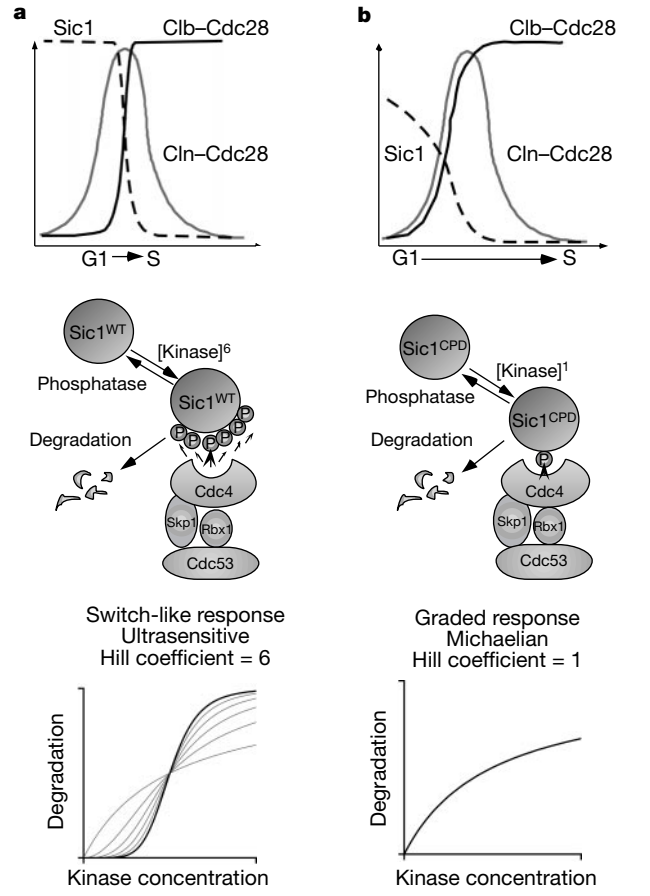

Figure 6 Ultrasensitivity at the G1/S transition. **a**, Multisite phosphorylation of Sic1 sets a threshold for Cln–Cdc28 activity and converts the increase in Cln–Cdc28 into a switch-like response for degradation of Sic1 and onset of Clb–Cdc28 activity. The requirement for six distributive phosphorylation events in Sic1 targeting creates an ultrasensitive response, as modelled by degradation = $([\text{kinase}]^{nH})/(K_m+[\text{kinase}]^{nH})$, with a Hill coefficient (nH) of six. K_m, Michaelis constant; [kinase], kinase concentration. The theoretical Hill plot shows the predicted response for 1, 2, 3, 4, 5 and 6 phosphorylation sites. **b**, A single, optimal CPD site suffices for efficient targeting of Sic1 to Cdc4, but only with michaelian kinetics (Hill coefficient = 1) and a hyperbolic response curve, which results in premature onset of degradation and uncoordinated activation of Clb5/6–Cdc28.

environment in which kinases and phosphatases act in dynamic equilibrium, a situation that lends itself to the generation of ultrasensitive biological responses[35]. The requirement for phosphorylation of Sic1 on at least six sites by definition introduces a highly cooperative step in the degradation pathway (Fig. 6). That is, the forward reaction rate to form the sextuply phosphorylated Sic1 varies as the sixth order of CDK kinase concentration, provided that phosphorylation occurs in a multi-hit distributive manner, as seems to be the case[46]. Additional factors may well enforce the switch-like elimination of Sic1, including inhibition of the phosphatase back-reaction upon Cdc4 binding, operation of CDK kinases at near saturation, and feed-forward action of liberated Clb5/6–Cdc28 on Sic1 (ref. 35). Quantitative measurements of Sic1 degradation rate as a function of relevant kinase, phosphatase, SCF and proteasomal activities should permit mathematical modelling of this crucial step in cell cycle progression, and allow further elucidation of the basis for switch-like biological responses. □

Methods

Yeast strain construction, culture growth, FACS analysis, fluorescence microscopy and plasmid mutagenesis were carried out by standard methods[38,47]. Strains, plasmids and oligonucleotides used are listed in Tables 1, 2 and 3 of the Supplementary Information. We carried out recombinant protein production, peptide synthesis, binding assays, kinase assays and ubiquitination reactions essentially as described[5,48]. Determination of the equilibrium-binding constant was by fluorescence polarization on a Beacon 2000 Fluorescence Polarization System (Pan Vera) at 22 °C using 5 nM fluorescein-labelled probes. Peptide arrays were constructed according to the Spots-synthesis method[26] and probed with 1 μM purified Cdc4–Skp1 complex. Complete details of all methods are provided in the Supplementary Information.

Received 22 June; accepted 12 August 2001.

1. Hershko, A. & Ciechanover, A. The ubiquitin system. *Annu. Rev. Biochem.* **67,** 425–479 (1998).
2. Varshavsky, A. Naming a targeting signal. *Cell* **64,** 13–15 (1991).
3. Tyers, M. & Jorgensen, P. Proteolysis and the cell cycle: with this RING I do thee destroy. *Curr. Opin. Genet. Dev.* **10,** 54–64 (2000).
4. Bai, C. *et al.* SKP1 connects cell cycle regulators to the ubiquitin proteolysis machinery through a novel motif, the F-box. *Cell* **86,** 263–274 (1996).
5. Skowyra, D., Craig, K. L., Tyers, M., Elledge, S. J. & Harper, J. W. F-box proteins are receptors that recruit phosphorylated substrates to the SCF ubiquitin-ligase complex. *Cell* **91,** 209–219 (1997).
6. Schwob, E., Bohm, T., Mendenhall, M. D. & Nasmyth, K. The B-type cyclin kinase inhibitor $p40^{SIC1}$ controls the G1 to S transition in *S. cerevisiae*. *Cell* **79,** 233–244 (1994).
7. Schneider, B. L., Yang, Q. H. & Futcher, A. B. Linkage of replication to start by the Cdk inhibitor Sic1. *Science* **272,** 560–562 (1996).
8. Feldman, R. M., Correll, C. C., Kaplan, K. B. & Deshaies, R. J. A complex of Cdc4p, Skp1p, and Cdc53p/cullin catalyzes ubiquitination of the phosphorylated CDK inhibitor Sic1p. *Cell* **91,** 221–230 (1997).
9. Verma, R. *et al.* Phosphorylation of Sic1p by G1 Cdk required for its degradation and entry into S phase. *Science* **278,** 455–460 (1997).
10. Nugroho, T. T. & Mendenhall, M. D. An inhibitor of yeast cyclin-dependent protein kinase plays an important role in ensuring the genomic integrity of daughter cells. *Mol. Cell. Biol.* **14,** 3320–3328 (1994).
11. Amati, B. & Vlach, J. Kip1 meets SKP2: new links in cell-cycle control. *Nature Cell Biol.* **1,** E91–E93 (1999).
12. Winston, J. T., Chu, C. & Harper, J. W. Culprits in the degradation of cyclin E apprehended. *Genes Dev.* **13,** 2751–2757 (1999).
13. Sheaff, R. J., Groudine, M., Gordon, M., Roberts, J. M. & Clurman, B. E. Cyclin E-CDK2 is a regulator of $p27^{Kip1}$. *Genes Dev.* **11,** 1464–1478 (1997).
14. Spruck, C. H., Won, K. A. & Reed, S. I. Deregulated cyclin E induces chromosome instability. *Nature* **401,** 297–300 (1999).
15. Maniatis, T. A ubiquitin ligase complex essential for the NF-κB, Wnt/Wingless, and hedgehog signaling pathways. *Genes Dev.* **13,** 505–510 (1999).
16. Yaron, A. *et al.* Identification of the receptor component of the IκBα-ubiquitin ligase. *Nature* **396,** 590–594 (1998).
17. Carrano, A. C., Eytan, E., Hershko, A. & Pagano, M. SKP2 is required for ubiquitin-mediated degradation of the CDK inhibitor p27. *Nature Cell Biol.* **1,** 193–199 (1999).
18. Tsvetkov, L. M., Yeh, K. H., Lee, S. J., Sun, H. & Zhang, H. $p27^{Kip1}$ ubiquitination and degradation is regulated by the SCF^{Skp2} complex through phosphorylated Thr187 in p27. *Curr. Biol.* **9,** 661–664 (1999).
19. Pawson, T. & Nash, P. Protein–protein interactions define specificity in signal transduction. *Genes Dev.* **14,** 1027–1047 (2000).
20. Drury, L. S., Perkins, G. & Diffley, J. F. The Cdc4/34/53 pathway targets Cdc6p for proteolysis in budding yeast. *EMBO J.* **16,** 5966–5976 (1997).
21. Lanker, S., Valdivieso, M. H. & Wittenberg, C. Rapid degradation of the G1 cyclin Cln2 induced by CDK-dependent phosphorylation. *Science* **271,** 1597–1601 (1996).
22. Schneider, B. L. *et al.* Yeast G1 cyclins are unstable in G1 phase. *Nature* **395,** 86–89 (1998).
23. Henchoz, S. *et al.* Phosphorylation- and ubiquitin-dependent degradation of the cyclin-dependent kinase inhibitor Far1p in budding yeast. *Genes Dev.* **11,** 3046–3060 (1997).
24. Clurman, B. E., Sheaff, R. J., Thress, K., Groudine, M. & Roberts, J. M. Turnover of cyclin E by the ubiquitin–proteasome pathway is regulated by Cdk2 binding and cyclin phosphorylation. *Genes Dev.* **10,** 1979–1990 (1996).
25. Won, K. A. & Reed, S. I. Activation of cyclin E/CDK2 is coupled to site-specific autophosphorylation and ubiquitin-dependent degradation of cyclin E. *EMBO J.* **15,** 4182–4193 (1996).
26. Frank, R. Spot-synthesis: an easy technique for positionally addressable, parallel chemical synthesis on a membrane support. *Tetrahedron* **48,** 9217–9232 (1992).
27. Songyang, Z. *et al.* Use of an oriented peptide library to determine the optimal substrates of protein kinases. *Curr. Biol.* **4,** 973–982 (1994).
28. Meimoun, A. *et al.* Degradation of the transcription factor Gcn4 requires the kinase Pho85 and the SCF^{CDC4} ubiquitin-ligase complex. *Mol. Biol. Cell* **11,** 915–927 (2000).
29. McKinney, J. D. & Cross, F. R. *FAR1* and the G1 phase specificity of cell cycle arrest by mating factor in *Saccharomyces cerevisiae*. *Mol. Cell. Biol.* **15,** 2509–2516 (1995).
30. Gartner, A. *et al.* Pheromone-dependent G1 cell cycle arrest requires Far1 phosphorylation, but may not involve inhibition of Cdc28-Cln2 kinase, *in vivo*. *Mol. Cell. Biol.* **18,** 3681–3691 (1998).
31. Yaffe, M. B. & Elia, A. E. Phosphoserine/threonine-binding domains. *Curr. Opin. Cell. Biol.* **13,** 131–138 (2001).
32. Wall, M. A. *et al.* The structure of the G protein heterotrimer Gi α1 β1 γ2. *Cell* **83,** 1047–1058 (1995).
33. Nishizawa, M., Kawasumi, M., Fujino, M. & Toh-e, A. Phosphorylation of Sic1, a cyclin-dependent kinase (Cdk) inhibitor, by Cdk including Pho85 kinase is required for its prompt degradation. *Mol. Biol. Cell* **9,** 2393–2405 (1998).
34. O'Neill, E. M., Kaffman, A., Jolly, E. R. & O'Shea, E. K. Regulation of PHO4 nuclear localization by the PHO80-PHO85 cyclin-CDK complex. *Science* **271,** 209–212 (1996).
35. Ferrell, J. E. Tripping the switch fantastic: how a protein kinase cascade can convert graded inputs into switch-like outputs. *Trends Biochem. Sci.* **21,** 460–466 (1996).
36. Cormack, B. Green fluorescent protein as a reporter of transcription and protein localization in fungi. *Curr. Opin. Microbiol.* **1,** 406–410 (1998).
37. Donovan, J. D., Toyn, J. H., Johnson, A. L. & Johnston, L. H. $P40^{SDB25}$, a putative CDK inhibitor, has a role in the M/G1 transition in *Saccharomyces cerevisiae*. *Genes Dev.* **8,** 1640–1653 (1994).

38. Spencer, F., Gerring, S. L., Connelly, C. & Hieter, P. Mitotic chromosome transmission fidelity mutants in *Saccharomyces cerevisiae*. *Genetics* **124,** 237–249 (1990).
39. Elsasser, S., Chi, Y., Yang, P. & Campbell, J. L. Phosphorylation controls timing of Cdc6p destruction: a biochemical analysis. *Mol. Biol. Cell* **10,** 3263–3277 (1999).
40. Drury, L. S., Perkins, G. & Diffley, J. F. The cyclin-dependent kinase Cdc28p regulates distinct modes of Cdc6p proteolysis during the budding yeast cell cycle. *Curr. Biol.* **10,** 231–240 (2000).
41. Wolf, D. A., McKeon, F. & Jackson, P. K. F-box/WD-repeat proteins Pop1p and Sud1p/Pop2p form complexes that bind and direct the proteolysis of Cdc18p. *Curr. Biol.* **9,** 373–376 (1999).
42. Chi, Y. *et al*. Negative regulation of Gcn4 and Msn2 transcription factors by Srb10 cyclin-dependent kinase. *Genes Dev.* **15,** 1078–1092 (2001).
43. Patton, E. E., Willems, A. R. & Tyers, M. Combinatorial control in ubiquitin-dependent proteolysis: don't Skp the F-box hypothesis. *Trends Genet.* **14,** 236–243 (1998).
44. Dirick, L., Goetsch, L., Ammerer, G. & Byers, B. Regulation of meiotic S phase by Ime2 and a Clb5,6-associated kinase in *Saccharomyces cerevisiae*. *Science* **281,** 1854–1857 (1998).
45. Cohen, P. The regulation of protein function by multisite phosphorylation: a 25 year update. *Trends Biochem. Sci.* **25,** 596–601 (2000).
46. Annan, R. S., Huddleston, M. J., Verma, R., Deshaies, R. J. & Carr, S. A. A multidimensional electrospray MS-based approach to phosphopeptide mapping. *Anal. Chem.* **73,** 393–404 (2001).
47. Guthrie, C. & Fink, G. R. (eds) *Methods in Enzymology* (Academic, San Diego, 1991).
48. van der Geer, P., Wiley, S., Gish, G. D. & Pawson, T. The Shc adaptor protein is highly phosphorylated at conserved, twin tyrosine residues (Y239/240) that mediate protein-protein interactions. *Curr. Biol.* **6,** 1435–1444 (1996).

Supplementary Information accompanies the paper on *Nature*'s website (http://www.nature.com).

Acknowledgements

We thank G. Gish for helpful discussions and initial peptide synthesis; A. Breitkreutz for assistance with phosphorylation reactions; A. Willems for assistance with modelling; and D. Durocher, A. Amon and L. Harrington for critical comments on the manuscript. This work was supported by grants from the Canadian Institutes of Health Research (CIHR), the National Cancer Institute of Canada (NCIC), the Protein Engineering Network of Centers of Excellence (PENCE) and MDS/Sciex (F.S., T.P. and M.T.), the Human Frontiers Science Program (M.T.), and from the National Institutes of Health (F.G. and M.D.M.). P.N. and X.T. are recipients of CIHR postdoctoral fellowship awards, T.P. is a Distinguished Scientist of the CIHR, M.T. is a Canada Research Chair in Biochemistry and F.S. is an NCIC Scientist.

Correspondence and requests for materials should be addressed to T.P. (e-mail: pawson@mshri.on.ca) or M.T. (e-mail: tyers@mshri.on.ca). The protein interactions are available at the Biomolecular Interaction Network Database (accession numbers 1436, 1437 and 1438).